Prospects of an alternative treatment against Trypanosoma cruzi based on abietic acic derivatives show promising results in Balb/c mouse model

ARTICLE *in* EUROPEAN JOURNAL OF MEDICINAL CHEMISTRY · JANUARY 2015

Impact Factor: 3.45 · DOI: 10.1016/j.ejmech.2014.11.004

10 AUTHORS, INCLUDING:

Clotilde Marin
University of Granada
76 PUBLICATIONS **625** CITATIONS
SEE PROFILE

Messouri Ibtissam
University of Granada
18 PUBLICATIONS **135** CITATIONS
SEE PROFILE

Kristina Urbanova
University of Granada
4 PUBLICATIONS **8** CITATIONS
SEE PROFILE

Manuel Sánchez-Moreno
University of Granada
141 PUBLICATIONS **1,338** CITATIONS
SEE PROFILE

European Journal of Medicinal Chemistry 89 (2015) 683–690

Contents lists available at ScienceDirect

European Journal of Medicinal Chemistry

journal homepage: http://www.elsevier.com/locate/ejmech

Original article

Prospects of an alternative treatment against *Trypanosoma cruzi* based on abietic acid derivatives show promising results in Balb/c mouse model

F. Olmo [a], J.J. Guardia [b], C. Marin [a], I. Messouri [b], M.J. Rosales [a], K. Urbanová [a], I. Chayboun [b], R. Chahboun [b], E.J. Alvarez-Manzaneda [b], M. Sánchez-Moreno [a, *]

[a] Department of Parasitology, Instituto de Investigación Biosanitaria ibs, University of Granada, Severo Ochoa s/n, E-18071 Granada, Spain
[b] Department of Organic Chemistry, University of Granada, Severo Ochoa s/n, E-18071 Granada, Spain

ARTICLE INFO

Article history:
Received 26 February 2014
Received in revised form
29 October 2014
Accepted 1 November 2014
Available online 3 November 2014

Keywords:
Anti-chagasic
Abietic acid
Chemotherapy
Trypanosomiasis

ABSTRACT

Chagas disease, caused by the protozoa parasite *Trypanosoma cruzi*, is an example of extended parasitaemia with unmet medical needs. Current treatments based on old-featured benznidazole (Bz) and nifurtimox are expensive and do not fulfil the criteria of effectiveness, and a lack of toxicity devoid to modern drugs. In this work, a group of abietic acid derivatives that are chemically stable and well characterised were introduced as candidates for the treatment of Chagas disease. *In vitro* and *in vivo* assays were performed in order to test the effectiveness of these compounds. Finally, those which showed the best activity underwent additional studies in order to elucidate the possible mechanism of action. *In vitro* results indicated that some compounds have low toxicity (i.e. >150 μM, against Vero cell) combined with high efficacy (i.e. <20 μM) against some forms of *T. cruzi*. Further *in vivo* studies on mice models confirmed the expectations of improvements in infected mice. *In vivo* tests on the acute phase gave parasitaemia inhibition values higher those of Bz, and a remarkable decrease in the reactivation of parasitaemia was found in the chronic phase after immunosuppression of the mice treated with one of the compounds. The morphological alterations found in treated parasites with our derivatives confirmed extensive damage; energetic metabolism disturbances were also registered by ^{1}H NMR. The demonstrated *in vivo* activity and low toxicity, together with the use of affordable starting products and the lack of synthetic complexity, put these abietic acid derivatives in a remarkable position toward the development of an anti-Chagasic agent.

1. Introduction

American trypanosomiasis is a potentially life-threatening parasitic disease caused by *Trypanosoma cruzi*. There are more than 10–20 million people infected worldwide, mostly in Latin America. Although not a uniform death sentence, *T. cruzi* infection is far from innocuous, as an estimated 30–40% of infected individuals develop debilitating and chronic disease, and this infection accounts for 20,000–50,000 deaths per year [1]. Currently, the available drugs used for the treatment of this infection, Benznidazole (Bz) or nifurtimox, show limited therapeutic potential and are associated with serious side effects, such as skin rashes, leucopoenia, neurotoxicity, fever, articular and muscular pain, peripheral neuropathy, lymphadenopathy, agranulocytosis, and thrombocytopenic purpura [2,3]. Thus, there is an urgent need for the development of new anti-trypanosomal agents with lower toxicity and greater activity, especially for the chronic phase of the disease. To date, no vaccine has been developed against *T. cruzi* [4]. Therefore, the search for new targets for chemotherapy and vaccines is a major challenge. Among the targets, the parasite antioxidant system has attracted attention due to its uniqueness in the trypanosomatids.

Antiprotozoal activity has been reported for some abietane diterpenoids. Thus, 5,6-didehydro-7-hydroxy-taxodone showed remarkable activity with acceptable selectivity against *Plasmodium falciparum* (IC_{50} 9.2 μM, SI 10.4 μM) and *Trypanosoma brucei* (IC_{50} 1.9 μM, SI 50.5 μM) [5]. 7-Hydroxy-12-methoxy-20-nor-abieta-1,5(10),7,9,12-pentaen-6,14-dione and abieta-8,12-dien-11,14-dione (12-deoxy-royleanone) showed appreciable *in vitro* anti-leishmanial activity against intracellular amastigote forms of both *Leishmania donovani* (IC_{50} values of 170 and 120 nM, respectively)

* Corresponding author.
E-mail address: msanchem@ugr.es (M. Sánchez-Moreno).

http://dx.doi.org/10.1016/j.ejmech.2014.11.004
0223-5234/

and *Leishmania major* (IC_{50} values of 290 and 180 nM, respectively) [6]. 12-Methoxycarnosic acid showed antiprotozoal activity against axenically grown *L. donovani* amastigotes with an IC_{50} of 0.75 μM with marginal cytotoxicity against the L6-cells (IC_{50}, 17.3 μM) [7]. The 20-*nor*-abietane diterpene komariviquinone showed strong trypanocidal activity against epimastigotes of *T. cruzi*, the causative agent of American Trypanosomiasis [8].

Taking into account this need for new drugs to combat *T. cruzi* parasites, we considered studying the activity of the abietic acid derivatives **1**–**5** against the causing agent of Chagas disease to be of great interest. These compounds are quite interesting, since their synthesis starts form cheap substrates and the procedures are not very complicated in most of the cases. In this work, their antiproliferative activity and unspecific mammalian cytotoxicity in the species considered were evaluated *in vitro*, and these measures were complemented by infectivity assays on Vero cells. Furthermore, those in whom *in vitro* activity showed remarkable effects were tested *in vivo*. Finally, the parasites were submitted to a thorough study of the possible mechanisms of action of the compounds assayed, as follows: (i) an ^1H NMR study concerning the nature and percentage of metabolite excretion was performed in order to obtain information on the inhibitory effect of the phenolic derivatives **1**–**5** on the glycolytic pathway, since it represents the primary source of energy for the parasite, (ii) alterations caused in the cell ultrastructure of the parasites were recorded using transmission electronic microscopy (TEM), and (iii) an enzymatic study of inhibition over the iron superoxide dismutase (Fe-SOD), which represent one of the many mechanisms of antioxidant defence in trypanosomatids.

2. Materials and methods

2.1. Chemistry

The abietane type diterpenes **1**–**4** and the podocarpane derivative **5** were synthesized starting from commercial abietic acid (Fig. 1). **1** (11-bromoferruginol), not yet found in nature, was obtained after bromination of ferruginol (12-hydroxy-abieta-8,11,13-triene), previously synthesized from abietic acid. **2**, (+)-sugiol is a natural terpene widely distributed in nature, which was isolated for the first time from *Juniperus communis* L. [9].

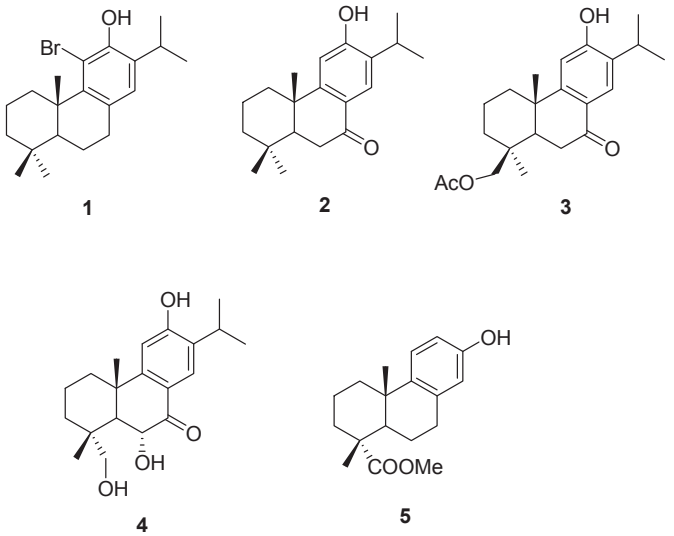

Fig. 1. Chemical structure of the 5 different compounds assayed: Phen **1**–**5**.

It has been prepared after a Friedel–Crafts acetylation of 8,11,13-abietatriene, Baeyer–Villiger oxidation of the resulting methyl ketone, benzylic oxidation of the obtained acetyloxy derivative and further deacetylation. The no natural terpene **3** and the abietane derivative **4**, (+)-fortunin E, isolated from *Cladonia fortunei* [10], have been synthesized starting from methyl 12-hydroxydehydroabietate, prepared from abietic acid [11]. **5**, the methyl ester of 13-hydroxypodocarpa-8,11,13-trien-18-oic acid, a constituent of the *Pinus massoniana* resin [12], has also been synthesized from abietic acid, via methyl 15-hydroxydehydroabietate [13].

2.2. Parasite strain culture

T. cruzi SN3 strain of IRHOD/CO/2008/SN3 was isolated from domestic Rhodnius prolixus; biological origin is Guajira (Colombia) [14]. Epimastigote forms were grown in axenic Grace's insect medium (Gibco) supplemented with 10% inactivated foetal bovine serum (FBS) at 28 °C in tissue-culture flasks, Roux flasks (Corning, USA) with a surface area of 75 cm^2, as described by Ref. [15].

2.3. Transformation of epimastigotes to metacyclic forms

Metacyclogenesis was induced by culturing a 5-day-old culture of epimastigote forms of *T. cruzi* that was harvested by centrifugation at 7000 g for 10 min at 10 °C according to [16].

2.4. Cell culture and cytotoxicity tests

Vero cells (Flow) were grown in RPMI and MEM (Gibco), supplemented with 10% iFBS and the procedure followed was as in Ref. [17].

2.5. In vitro activity assays, extracellular forms

2.5.1. Epimastigotes assay

T. cruzi epimastigotes were collected in the exponential growth phase and distributed in culture trays (with 24 wells) at a final concentration of 5×10^4 parasites/well. The effects on the parasite growth were tested according to [17].

2.5.2. Blood trypomastigote forms assay

Compounds **4**–**5** were also evaluated in blood trypomastigote forms of *T. cruzi*. BALB/c female mice infected with *T. cruzi* were used 7 days after infection. Blood was obtained by cardiac puncture using 3.8% sodium citrate as an anticoagulant in a 7:3 blood:-anticoagulant ratio. The parasitaemia in the infected mice was about 1×10^5 parasites/mL. The compounds were diluted in phosphate-buffered saline solution (PBS) to give a final concentration 10, 25, and 50 μM for each product. Aliquots (20 μL) of each solution were mixed in culture trays (96 wells) with 55 μL of infected blood containing the parasites at a concentration of approximately 1×10^6 parasites/mL. Infected blood with PBS, at the same concentrations as the products, was used as control. The plates were shaken for 10 min at room temperature and kept at 4 °C for 24 h. Each solution was examined microscopically (Olympus CX41) for parasite counting using the Neubauer haemocytometric chamber (a dilution of 1:100 in PBS was necessary to get into the range of counting). The activity (percent of parasites reduction) was compared with that of the control.

2.6. In vitro activity assays, intracellular forms: amastigotes assay

Vero cells were cultured in RPMI medium supplemented with 10% iFBS, in a humidified 95% air and 5% CO_2 atmosphere at 37 °C. Then the cells were infected and treated as in Ref. [15].

2.7. Infectivity assay

Vero cells were cultured in RPMI medium supplemented with 10% iFBS as described above. Afterward, the cells were infected *in vitro* with metacyclic trypomastigote forms of *T. cruzi* at a ratio of 10:1. The assay was performed as in Ref. [15].

2.8. In vivo trypanosomicidal activity assay

2.8.1. Mice infection and treatment

This experiment was performed using the rules and principles of the International Guide for Biomedical Research in Experimental Animals and with the approval of the ethical committee of the University of Granada, Spain. Groups of six BALB/c albino female mice (6–8 weeks old, 25–30 g weight), maintained under a 12-h dark/light cycle (lights on at 07:30 h) at a temperature of 22 ± 3 °C and provided with water and standard chow *ad libitum*, were inoculated via the intraperitoneal route with 5×10^5 blood trypomastigotes of *T. cruzi* obtained from previously infected mice blood. The animals were divided as follows: I, positive control group (mice infected but not treated); II, study group (mice infected and treated with the compounds under study). The administration of the testing compounds was begun on the seventh day of infestation once the infection was confirmed, and doses of 5 mg/kg body mass per day were used for 5 consecutive days (7–12 days post-infection). Peripheral blood was obtained from the mandibular vein of each mouse (5 μL samples) and dissolved in 495 μL of a PBS solution at a dilution of 1:100. The circulating parasite numbers were quantified with a Neubauer's chamber for counting blood cells. This counting was performed every 3 days during a 40 day period (acute phase). The number of bloodstream forms was expressed as parasites/mL.

2.8.2. Cyclophosphamide-induced immune suppression and assessment of cure

After day 60, the animals entered the chronic phase of the experiment where parasitaemia showed progressively decreasing levels independent of the treatment. Therefore, on day 120, parasitaemia was shown to be undetectable by fresh blood microscopic examination, and the mice received 4 intraperitoneal injections of 200 mg/kg of body mass of cyclophosphamide monohydrate (CP) (ISOPAC®) on alternate days, as previously described [18]. Within 1 week of the last CP injection, parasitaemia was evaluated according to the procedure described for acute phase to quantify the presence of blood trypomastigote forms as reactivation rate. Finally, mice were bled out, under gaseous anaesthesia (CO_2), via heart puncture and blood was collected. Blood was incubated for 2 h at 37 °C and then over night at 4 °C in order to allow clotting and then the serum was obtained from samples after centrifuging the supernatant twice at 1000 and 2700 g, consecutively. The serum was aliquoted and used for ELISA and biochemical analysis, as explained below. Hearts were harvested and immediately flushed free of blood by gentle infusion of 10 mL of pre-warmed PBS through the left ventricle [19] in order to avoid contamination of the collected tissue

Table 1
In vitro activity, toxicity and selectivity index found for Phen **1**–**5** and the reference drug on extracellular and intracellular forms of *Trypanosoma cruzi*.

Compounds	IC_{50} (μM)[a]			Toxicidad IC_{50} Vero cell (μM)[b]	IS[c]		
	Epimastigote forms	Intracellular amastigote forms	Trypomastigote forms		Epimastigote forms	Intracellular amastigote forms	Trypomastigote forms
Bz	15.9 ± 1.1	23.3 ± 4.6	16.4 ± 3.2	13.6 ± 0.9	0.8	0.6	0.8
1	49.7 ± 3.5	41.9 ± 8.1	nd	183.6 ± 12.2	3.69 (5)	4.38 (7)	nd
2	33.1 ± 3.6	24.6 ± 2.2	nd	45.4 ± 6.1	1.37 (2)	1.84 (3)	nd
3	26.3 ± 1.9	25.5 ± 1.6	nd	72.7 ± 7.7	2.8 (3)	2.8 (5)	nd
4	18.7 ± 0.9	7.1 ± 0.3	59.88 ± 0.7	221.6 ± 13.5	11.85 (15)	31.4 (52)	3.7 (5)
5	39.2 ± 3.8	27.1 ± 1.1	89.3 ± 1.1	473.6 ± 22.1	12.1 (15)	17.46 (29)	5.3 (7)

[a] IC_{50} = the concentration required to give 50% inhibition, calculated by linear regression analysis from the K_c values at concentrations employed (1, 10, 25, 50 and 100 μM).
[b] Towards cell Vero after 72 h of culture.
[c] Selectivity index = IC_{50} cell Vero/IC_{50} extracellular and intracellular form of parasite. In brackets: number of times that compound SI exceeds the reference drug SI. Results are averages of three separate determinations.

Table 2
Summarizes the biochemical clinical parameters tested in different groups of Balb/c mice infected with *Trypanosoma cruzi* at different experimental situations.

	Kidney markers profile		Heart markers profile		Liver markers profile			
	Urea (mg/dL)	Uric acid (mg/dL)	CK-MB (U/L)	LDH (U/L)	AST/GOT (U/L)	ALT/GPT (U/L)	Total bilirubin (mg/dL)	Alkalyne phosphatase (U/L)
Uninfected mice ($n = 15$)	39 [36–43]	5 [4.3–5.5]	453 [215–690]	3086 [2108–4064]	126 [103–148]	46 [37–54]	0.23 [0.17–0.28]	133 [104–161]
Infected mice-acute phase ($n = 15$)	49 [39–60]	4.5 [3.7–5.5]	681 [400–950]	2910 [1589–4232]	129 [100–157]	48 [38–58]	0.15 [0.12–0.18]	231 [161–300]
120 days post-infection mice ($n = 6$)	49 ± 12	4.3 ± 1.1	800 ± 45	2536 ± 765	148 ± 18	53 ± 9	0.12 ± 0.04	186 ± 45
120 days post-infection mice and 4 25 mg/kg of body mass treated ($n = 6$)	=	=	=	+	+	=	=	=
120 days post-infection mice and 5 25 mg/kg of body mass treated ($n = 6$)	=	-	- -	=	=	=	=	=

Key: =, variation no larger than 10%; +, up to 10% of increasing over the range; ++, up to 30% of increasing over the range; +++, up to 40% of increasing over the range; ++++, more than 50% of increasing over de range; -, up to 10% of decreasing over the range; - -, up to 30% of decreasing over the range; - - -, up to 40% of decreasing over the range; - - - -, more than 50% of decreasing over de range.

with blood parasites. After this, samples were frozen at −80 °C and stored until used for DNA extraction.

2.8.3. ELISA tests

Fe-SOD excreted from the parasite, cultured and processed as described in Ref. [20], was used as the antigen fraction. The ELISA test to measure the antibodies against *T. cruzi* used was performed as in Ref. [21].

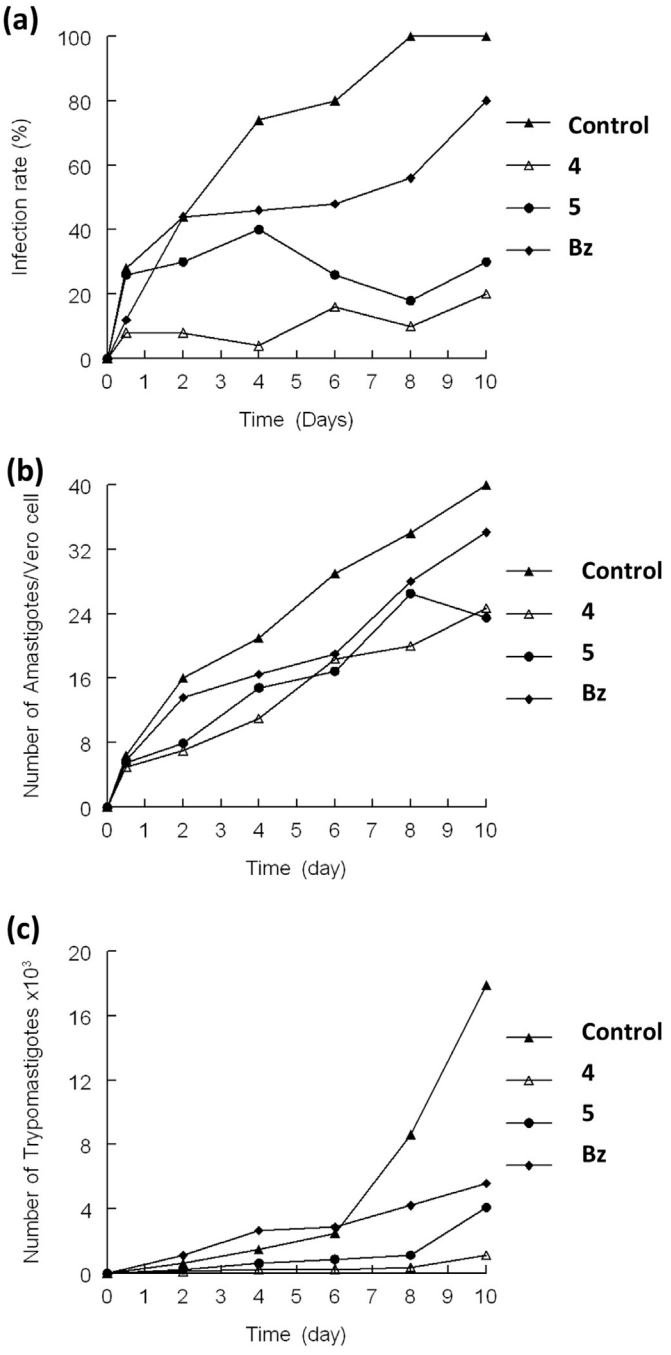

Fig. 2. Reduction of the infectivity of *T. cruzi* in Vero cells treated with **4**, **5** and Bz. (a) Rate of infection, (b) mean number of amastigotes per infected Vero cell and (c) number of trypomastigotes in the culture medium. Control group is represented with filled triangles; filled rhombuses represent Bz; open triangles represent **4**; **5** is represented by filled circles. Measured at IC_{25}. Values are the means of three separate experiments.

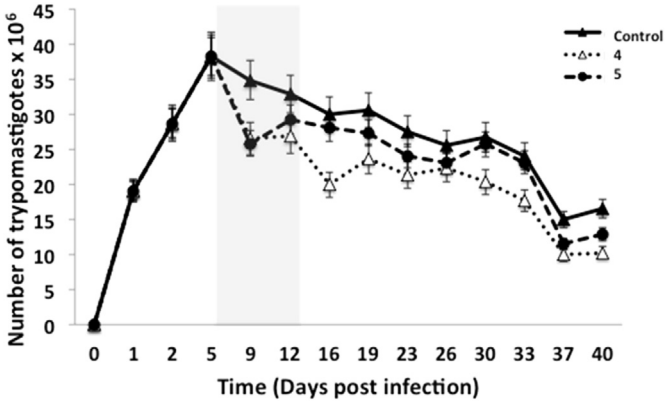

Fig. 3. Parasitaemia in the murine model of acute Chagas disease: filled triangles represent control, open triangles and filled circles represent group treated with **4** and **5**, respectively, with a final dose received of 25 mg/kg of body mass administered by the intraperitoneal route. Grey shade represents the treatment days.

2.8.4. DNA extraction and PCR

Hearts were defrosted and then ground using a Potter-Elvehjem to follow the purification procedure of the Wizard® Genomic DNA Purification Kit (Promega). PCR was performed using two primers designed in our laboratory (unpublished data), based on the published sequence of the enzyme superoxide dismutase *T. cruzi* CL Brenner (GenBank accession No. XM_808937), which amplifies a fragment of approximately 300 bp belonging to the superoxide dismutase gene b of *T. cruzi*. The PCR was run in a total volume of 20 μL. Next, the amplification products were subjected to electrophoresis on 1.6% agarose gel containing 1:10,000 GelRed™ Nucleic Acid Gel Stain, for 90 min at 90 V.

2.8.5. Toxicity tests by clinical chemistry measurements

A fraction of the serum obtained as it was shown above was send to the Biochemical service in the University of Granada where a series of parameters were measured according to their commercial kits

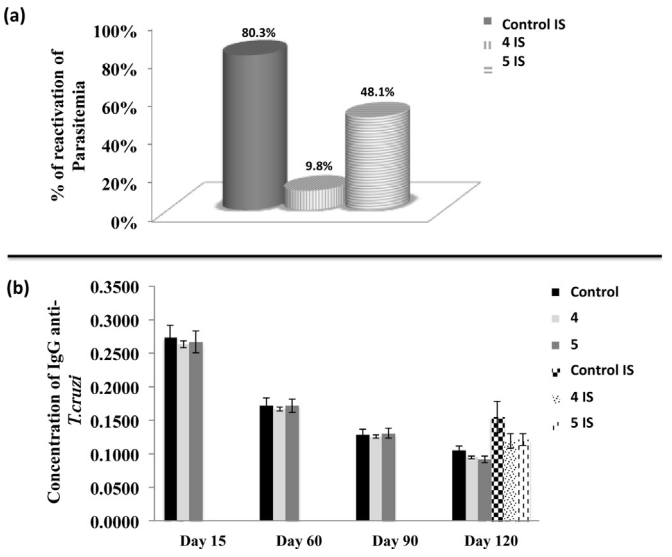

Fig. 4. Immunosuppression *in vivo* assay for mice untreated and treated with 25 mg/kg of body mass of **4** and **5**. (a) Shows the reactivation of blood parasitaemia after the immunesuppression cycles by fresh blood counting comparing to the peak day of parasitemia during acute phase. (b) Shows differences in the Ig G levels measured by ELISA at different day post-infection for immunosuppressed and non-immunosuppressed group of mice.

acquired from Cromakit® by BS-200 Chemistry Analyzer Shenzhen Mindray (Bio-medical Electronics Co., LTD). With the levels obtained for different populations of sera ($n = 15$, $n = 6$) we calculated the mean value and standard deviation. Finally, we also calculated the confidence interval for the mean normal populations based on a confidence level of 95% ($100 \times (1 - \alpha) = 100 \times (1 - 0.05)\%$). The ranges obtained are shown in Table 2, which allows comparison and analysis of the sera studied in this work.

2.9. Assays to figure out the mechanism of action

2.9.1. Metabolite excretion

Cultures of *T. cruzi* epimastigote forms (initial concentration of 5×10^5 cells/mL) received IC_{25} of the compounds (except for the control cultures). After incubation for 96 h at 28 °C, the cells were centrifuged at 400 g for 10 min. The supernatants were collected in order to determine the excreted metabolites through ^1H NMR, and the chemical shifts were expressed in parts per million (ppm), using dimethyl sulphoxide (DMSO) as the reference signal. One-dimensional ^1H NMR spectra were acquired on VARIAN DIRECT DRIVE 400 MHz Bruker spectrometer with AutoX probe using D_2O. The assignments of metabolites were based on 1D NMR spectrum. The chemical shifts used to identify the respective metabolites were consistent with those described previously by our group [22]. In addition, the human metabolome database (http://www.hmdb.ca/) was also used for this purpose. The spectral region of 1.0–5.5 ppm was bucketed into a frequency window of 0.1 ppm. The region corresponding to water (4.5–5.5 ppm) was excluded during binning to avoid artefacts due to pre-saturation of water, and the region corresponding to glucose (3.4–3.8 ppm) was also excluded. The aromatic region was excluded because the signal to noise ratio in this region was poorer compared to that of the aliphatic region. The peak (2.6 ppm) corresponding to DMSO was removed before binning. The resulting integrals were normalised to the working region (1.0–3.4) ppm of the spectrum to correct for inter-sample differences in dilution. The binning and normalisations were achieved using Mestrenova 9.0 software. The matrix obtained in Mestrenova was imported to Microsoft Excel for further data analyses.

2.9.2. Ultrastructural alterations

The parasites were cultured at a density of 5×10^5 cells/mL in each corresponding medium containing the compounds tested at the concentration of IC_{25}. After 96 h, these cultures were centrifuged at 400 g for 10 min and the pellets produced were washed in PBS before being mixed with 2% (v/v) paraformaldehyde/glutaraldehyde in 0.05 M cacodylate buffer (pH 7.4) for 24 h at 4 °C. Following this, the pellets were prepared for transmission electron microscopy study using a technique described by our group [15].

2.9.3. Superoxide dismutase inhibition assay

The parasites cultured as described above were centrifuged. The pellet was suspended in 3 mL of STE buffer (0.25 M sucrose, 25 mM Tris–HCl, 1 M EDTA, pH 7.8) and disrupted by three cycles of sonic disintegration, 30 s each at 60 W. The sonicated homogenate was centrifuged at 1500 g for 5 min at 4 °C, and the pellet was washed three times in ice-cold STE buffer. This fraction was centrifuged (2500 g for 10 min at 4 °C) and the supernatant was collected. The protein concentrations were determined using the Bradford method [23]. Iron and copper–zinc superoxide dismutases (Fe-SOD and CuZn-SOD) activities were determined using the method described by Beyer and Fridovich [24].

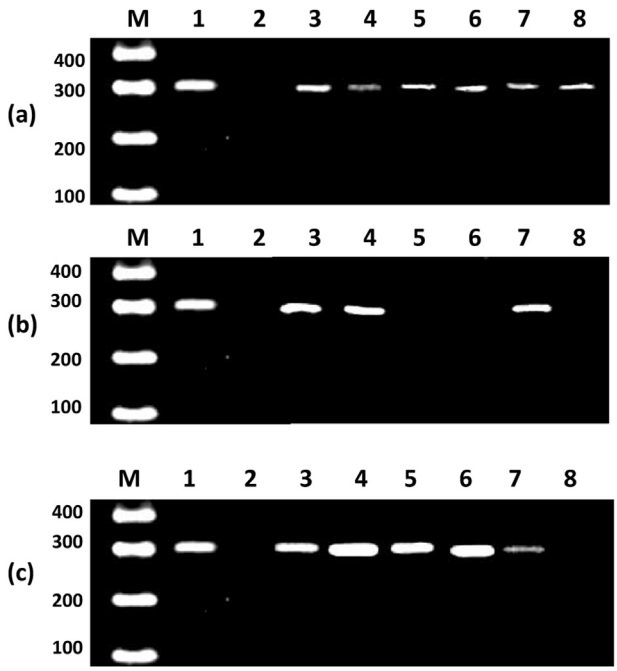

Fig. 5. Polymerase chain reaction (PCR) analysis of heart tissue at the day final day of experiment. (a) Shows untreated mice group, (b) Shows the group of mice treated with **4**, (c) Shows the group of mice treated with **5**. Lanes: M, base pair marker; 1, PCR positive control; 2, PCR negative control; 3–5, Non-immunosuppressed mice group; 6–8, Immunosuppressed mice group.

3. Results and discussion

3.1. In vitro trypanosomicidal evaluation

In order to get preliminary information, *in vitro* activities of **1**–**5** were evaluated against epimastigote, amastigote and trypomastigote forms of *T. cruzi*, as shown in Table 1. It was found that the more sensitive forms to all different compounds tested were the intracellular forms (amastigotes) reaching an effectiveness of 52 times higher than the reference drug in the case of **4**. The activity of **5** was also remarkable once again against the amastigote forms, being 29-fold more active than Bz. The rest of the compounds also showed trypanosomicidal activity against the different forms of the parasite and the effect was always better than that of the reference drug; however, they all showed less than 15 times effectiveness compared with Bz. As a result, these two compounds were chosen to undergo an extra *in vitro* assay and deeper insight of the activity of these compounds was found in the infectivity assay, where the

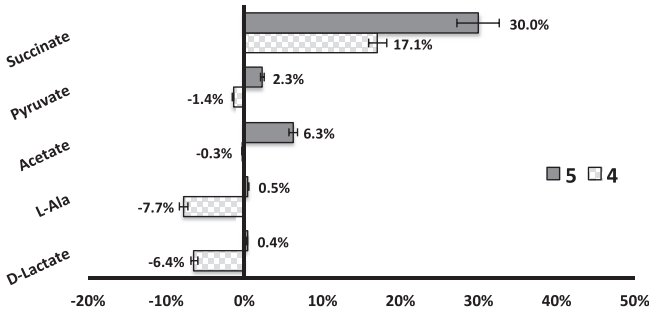

Fig. 6. Variation percentages in the height of the peaks corresponding to catabolites excreted by *T. cruzi* epimastigotes in the presence of **4** and **5** at their IC_{25}, compared to a control sample after 96 h of incubation.

process that takes place in the host of the lifecycle of *T. cruzi* in the presence of the drugs was reproduced *in vitro*. Once again, **4** was found to be the more active, decreasing the rate of infection in cells by 80% on the last day of the experiment, as shown in Fig. 2(a). It also decreased the average number of amastigote forms found per infected cell; these decreases reached the 38% for cells treated with **4** and 41% for those which received **5** as a treatment. Both cases were more efficient than Bz, which effectively only decreased the number by 15% compared to the control (Fig. 2(b)). The last data obtained from this assay were regarding the number of trypomastigote forms released by the infected cells; this effect was remarkable for both compounds, as can be seen in Fig. 2(c), where the effect showed a significant decrease of more than 75% for both compounds compared to the control assay.

3.2. *In vivo trypanosomicidal evaluation*

Since compounds **4** and **5** showed remarkable SI values with respect to Bz in the *in vitro* experiments, they were selected according to the criteria established by Ref. [25] for further *in vivo* studies in the chosen murine model. Their trypanozidal activity during the acute phase of Chagas disease [until 40 days post-infection (pi)] was first investigated. None of the animals treated with either the control or compounds **4** and **5** died during the treatment. As shown in Fig. 3, the reduction of parasitaemia in mice treated with compounds was evident from the very beginning of the treatment and was maintained until the end, resulting in parasitaemia reduction values of 45% and 22% with respect to the control experiment for **4** and **5**, respectively. Although Bz data have not been included in Fig. 3 for easier visualisation, it must be noted that parasitaemia reductions originated by Bz at the dose of 5 mg/kg body mass were much smaller (16.7% on day 40 pi).

The next step was to evaluate the behaviour of the two compounds until the chronic phase. Therefore, the mice treated as described above were taken up to day 120 pi (advanced chronic phase), in order to evaluate the immune status and the disease extent of the mice at that stage; blood samples were extracted for determining parasitaemia and immunoglobulin G (Ig-G) levels in comparison with the corresponding non-immunosuppressed (control) subgroup of mice (Fig. 4). Concerning the parasitaemia reactivation, Fig. 4(a) shows a very illustrative three-dimensional graph indicating the percentage of parasitaemia reactivation for **4** and **5** in comparison with the control mice; very low percentages were obtained in the two cases, with values ranging from 9.8% to 48.1%, whereas a reactivation of 80.3% was found in the control mice. Bz data obtained from the 80% mice that survived after treatment gave a substantially higher parasitaemia reactivation of 36% at 5 mg/kg of body mass, indicating that one of the tested compounds was clearly more efficient than the reference drug.

The enzyme-linked immunosorbent assay (ELISA) was used for the detection of total Ig-G levels and the antigen source was the Fe-SOD enzyme isolated in our laboratory. The detection of total Ig G

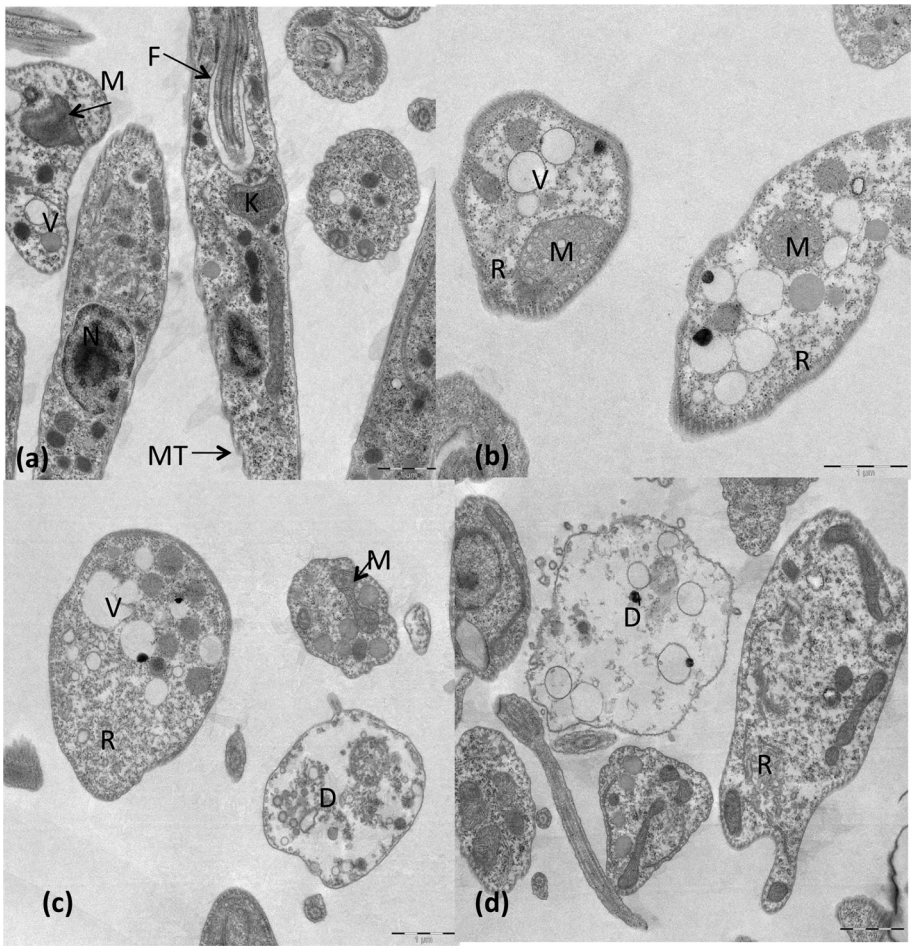

Fig. 7. Ultrastructural alterations shown by TEM in epimastigotes of *T. cruzi* treated with Phen **4** and **5** at IC_{25} concentration. (a) Control parasite showing typical organelles such as nucleus (N), mitochondrions (M), glycosomes (G), microtubules (MT), vacuoles (V), reservosomes (R), kinetoplast (K) and flagellum (F). (b) Treated with **4**. (c–d) Treated with **5**. Scale bar = 1 μm.

allowed evaluation of the immune status of the mice [26], since that indicates the level of protection that should be attributed to the tested compounds, combined with the innate protection that mice have naturally [27]. Results obtained from the ELISA experiments were confirmed by the parasitaemia assay performed as indicated above. In accordance with the ELISA test, the group of mice treated with compounds **4** and **5** maintained levels of total Ig G (Fig. 4(b)), as did chronic infected mice, lower than that of the control group after being immunosuppressed, while the control group levels were increased as a consequence of the reactivation of parasitaemia. Finally, Fig. 5 shows the PCR results after necropsy. After removing the hearts, performing total DNA extraction and amplification of a fragment within the parasite SOD-gene, the hearts of control animals showed the ubiquitous presence of the parasite. In striking contrast, hearts in mice treated with **4** were relatively free from parasites (50%), thus confirming the partial curative effect of this compound at the studied dosage. Less significant was the effect of **5**, where only around the 17% of mice were free of parasites.

Clinical chemistry measurements are provided in Table 2. Changes in lactate dehydrogenase (LDH) and aspartate aminotransferase (AST) for the group of mice treated with **4** were the only differences found when compared to the control group, but these changes were insignificant since they were lower than 10%. This confirms the evidence that the compounds tested are not toxic in the murine model; in fact, this lack of toxicity added to the better efficacy of **4**, leading us consider this compound as a promising candidate for the treatment of Chagas disease. Therefore, the compound should be followed-up in future clinical experiments.

3.3. Possible mechanism of action

Trypanosomatids are unable to completely degrade glucose to CO_2, so they excrete part of the hexose skeleton into the medium as partially oxidised fragments, the nature and percentage of which depend on the pathway used for glucose metabolism [28]. The catabolism products in *T. cruzi* are mainly succinate, acetate, D-lactate and L-alanine [29]. In order to obtain some information about the effects of **4** and **5** on the glucose metabolism of the parasite, we registered the ^{1}H NMR spectra of *T. cruzi* epimastigotes treated with the test compounds (spectra not shown); the final excretion products were identified qualitatively and quantitatively, and the results obtained were compared with those found for untreated control epimastigotes. Fig. 6 shows the differences found in every case with respect to the control.

Excretion of all metabolites was disturbed in the treatment with **5**, with succinate being the most affected, showing an increase of 30%, followed by acetate and pyruvate with increases of 6.3 and 2.3%, respectively. In general, all metabolites were increased in the medium when the parasites were treated with **5**. However, changes were notably less significant with **4** than **5**. In this case, all of the metabolites, with the exception of succinate, were slightly decreased. L-alanine and D-Lactate showed the most remarkable decreases of 7.7% and 6.4%, respectively. On the other hand, succinate was also disturbed and, as seen with **5**, it was overexpressed in the medium at 17.1%. All of these data could be interpreted on the basis of a change in the succinate, D-lactate, L-alanine pathways occurring in the presence of the compounds under investigation. It is well known that D-lactate and L-alanine originate from the transformation of PEP in pyruvate in the presence of pyruvate kinase or pyruvate phosphate dikinase [30]. On the other hand, it is interesting to note that the increase in succinate with **5** indicate catabolic changes that could be related to a malfunction of the mitochondria, due to the redox stress produced by inhibition of the mitochondrion-resident Fe-SOD enzyme [31], which should result in decreased pyruvate metabolism and a consequent decrease of the succinate produced in mitochondria. Overall, these data should confirm that the modifications generated in organelles like glycosomes or mitochondria by the compounds assayed are the ultimate reason for the alterations observed in the excreted products of *T. cruzi*.

Modifications at the ultrastructural level caused after incubation of epimastigote forms of *T. cruzi* with the compounds under study in the current work, **4** and **5**, have been studied. Both compounds induced strong disturbances in the parasites' morphology and consequently death in some cases. At this level, **5** was found to be the more effective compound, causing more mortality in the parasite cultures compared to **4** when the IC_{25} was administered. Although the survival rate was higher in parasites treated with **4**, the parasites were clearly morphologically disturbed when compared with the untreated assay, as shown in Fig. 7(a). Among the more common disturbances when **4** was added to the medium, as shown in Fig. 7(b), include the finding that mitochondria were swollen, without cristae and almost unrecognisable; the cytoplasm was also full of small vacuoles, there was a lack of ribosomes and low electron density was appreciated. Fig. 7(c) and (d) reveal the aspect of parasites that survived after treatment with **5**, where the most frequent change was vacuolisation with enormous empty

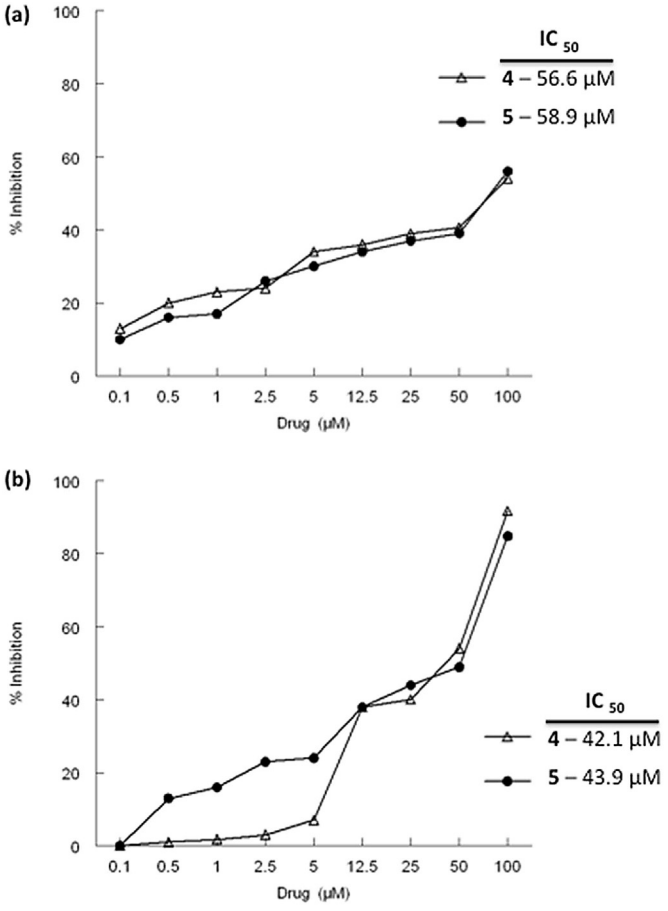

Fig. 8. (a) *In vitro* inhibition (%) of CuZn-SOD from human erythrocytes for compounds (activity 23.36 ± 4.21 U/mg). (b) *In vitro* inhibition (%) of Fe-SOD from *T. cruzi* epimastigotes for compounds (activity 20.77 ± 3.18 U/mg). Differences between the activities of the control homogenate and those ones incubated with compounds were obtained according to the Newman–Keuls test. Values are the average of three separate determinations.

vacuoles and swollen mitochondria combined with the low electron density and a lack of ribosomes, as seen with **4**.

These results prompted us to evaluate the inhibitory effect of compounds **4** and **5** on SOD activity to test their potential as enzyme inhibitors. The results obtained are shown in Fig. 8, with the corresponding IC_{50} values that were calculated. Significant inhibitory values of Fe-SOD activity were found for the two tested compounds (Fig. 8(b)). Compounds **4** and **5** showed values close to 100% inhibition at 80 μM, with IC_{50} values between 42.1 and 43.9 μM. The design of an effective drug that is able to inhibit parasite Fe-SOD without inhibiting human Cu/Zn-SOD is an interesting goal. Therefore, we also assayed the effect of compounds on Cu/Zn-SOD in human erythrocytes (Fig. 8(a)). The results obtained showed that the inhibition percentages for human Cu/Zn-SOD were lower than for Fe-SOD. Therefore, IC_{50} values of 56.6 and 58.9 μM were reached in Cu/Zn-SOD for **4** and **5**, respectively.

Acknowledgements

F.O. is grateful for a FPU Grant (AP-2010-3562) from the Ministry of Education of Spain. I. C. thanks the Spanish Agency for the International Development and Cooperation (AECID) for a predoctoral grant.

References

[1] R.L. Tarleton, J.W. Curran, Is Chagas disease really the "new HIV/AIDS of the Americas"? PLoS Negl. Trop. Dis. 6 (2012) e1861.
[2] J.A. Urbina, Specific chemotherapy of Chagas disease: relevance, current limitations and new approaches, Acta Trop. 115 (2010) 55–68.
[3] S.R. Wilkinson, M.C. Taylor, D. Horn, et al., A mechanism for cross-resistance to nifurtimox and Bz in trypanosomes, Proc. Natl. Acad. Sci. 105 (2008) 5022–5027.
[4] E. Dumonteil, Vaccine development against Trypanosoma cruzi and Leishmania species in the post-genomic era, Infect. Genet. Evol. 9 (2009) 1075–1082.
[5] Ramzi A. Mothana, Mansour S. Al-Said, Nawal M. Al-Musayeib, Ali A. El Gamal, Shaza M. Al-Massarani, Adnan J. Al-Rehaily, Majed Abdulkader, Louis Maes, Int. J. Mol. Sci. 15 (2014) 8360–8371.
[6] Nur Tana, Macki Kalogaa, Oliver A. Radtkea, Albrecht F. Kiderlenc, Sevil Oksuz, Ayhan Ulubelenb, Herbert Kolodzieja, Phytochemistry 61 (2002) 881–884.
[7] Tsholofelo A. Mokoka, Xolani K. Peter, Gerda Fouche, Nivan Moodley, Michael Adams, Matthias Hamburger, Marcel Kaiser, Reto Brun, Vinesh Maharaj, Neil Koorbanally, South Afr. J. Bot. 90 (2014) 93–95.
[8] Nahoko Uchiyama, Fumiyuki Kiuchi, Michiho Ito, Gisho Honda, Yoshio Takeda, Olimjon K. Khodzhimatov, Ozodbek A. Ashurmetov, J. Nat. Prod. 66 (2003) 128–131.
[9] J.B.S. Bredenberg, J. Gripenberg, The chemistry of the natural order Cupressales. XIII. The presence of sugiol in the wood of Juniperus communis, Acta Chem. Scand. 8 (1954) 1728.
[10] S. Yao, C.P. Tang, C.Q. Ke, et al., Abietane diterpenoids from the bark of Cryptomeria fortunei, J. Nat. Prod. 71 (2008) 1242–1246.
[11] E.J. Alvarez-Manzaneda, R. Chahboun, E. Alvarez, et al., Synthesis of (+)-hanagokenol A, (+)-fortunins E, G, H, and (−)-sugikurojin A from abietic acid, Synthesis (2010) 3493–3503.
[12] H.T.A. Cheung, T. Miyase, M.P. Lenguyen, et al., Further acidic constituents and neutral components of Pinus massoniana resin, Tetrahedron 49 (1993) 7903–7915.
[13] E.J. Alvarez-Manzaneda, R. Chahboun, J.J. Guardia, et al., New route to 15-hydroxydehydroabietic acid derivatives: application to the first synthesis of some bioactive abietane and nor-abietane type terpenoids, Tetrahedron Lett. 47 (2006) 2577–2580.
[14] J. Tellez-Meneses, A.M. Mejía-Jaramillo, O. Triana-Chavez, Biological characterization of Trypanosoma cruzi stocks from domestic and sylvatic vectors in Sierra Nevada of Santa Marta, Colombia, Acta Trop. 108 (2008) 26–34.
[15] P. González, C. Marín, I. Rodríguez-González, A.B. Hitos, et al., In vitro activity of C20-diterpenoid alkaloid derivatives in promastigotes and intracellular amastigotes of Leishmania infantum, Int. J. Antimicrob. Agents 25 (2005) 136–141.
[16] J. Cardoso, M.J. Soares, In vitro effects of citral on Trypanosoma cruzi metacyclogenesis, Mem. Inst. Oswaldo Cruz 5 (2010) 1026–1032.
[17] R. Magán, C. Marín, M.J. Rosales, et al., Therapeutic potential of new Pt(II) and Ru(III) triazole-pyrimidine complexes against Leishmania donovani, Pharmacology 73 (2005) 41–48.
[18] S. Cencig, N. Coltel, C. Truyens, et al., Parasitic loads in tissues of mice infected with Trypanosoma cruzi and treated with AmBisome, PLoS Negl. Trop. Dis. 5 (2011) e1216.
[19] X. Ye, J. Ding, X. Zhou, et al., Divergent roles of endotelial NF-kappaB in multiple organ injury and bacterial clearance in mouse models of sepsis, J. Exp. Med. 205 (2008) 1303–1315.
[20] A. Lopez-Cespedes, E. Villagran, K. Briceño-Alvarez, et al., Trypanosoma cruzi: seroprevalence detection in suburban population of Santiago de Queretaro (Mexico), Sci. World J. (2012), http://dx.doi.org/10.1100/2012/914129.
[21] F. Olmo, C. Rotger, I. Ramírez-Macías, L. Martínez, C. Marín, L. Carreras, K. Urbanová, M. Vega, G. Chaves-Lemaur, A. Sampedro, M.J. Rosales, M. Sánchez-Moreno, A. Costa, Synthesis and biological evaluation of N,N′-squaramides with high in vivo efficacy and low toxicity: toward a low-cost drug against Chagas disease, J. Med. Chem. 57 (3) (2014 Feb 13) 987–999.
[22] C. Fernandez-Becerra, M. Sanchez-Moreno, A. Osuna, et al., Comparative aspects of energy metabolism in plant trypanosomatids, J. Eukaryot. Microbiol. 44 (1997) 523–529.
[23] M.M. Bradford, A refined and sensitive method for the quantification of microgram quantities of protein utilizing the principle of protein-dye binding, Anal. Biochem. 72 (1972) 248–254.
[24] W.F. Beyer, I. Fridovich, Assaying for superoxide dismutase activity: some large consequences of minor changes in conditions, Anal. Biochem. 161 (1987) 559–566.
[25] S. Nwaka, D. Besson, B. Ramirez, et al., Integrated dataset of screening hits against multiple neglected disease pathogens, PLoS Negl. Trop. Dis. 5 (2011) e1412.
[26] A. El Bouhdidi, C. Truyens, M.T. Rivera, et al., Trypanosoma cruzi infection in mice induces a polyisotypic hypergammaglobulinaemia and parasite-specific response involving high IgG2a concentrations and highly avid IgG1 antibodies, Parasite Immunol. 16 (1994) 69–76.
[27] H. Kayama, K. Takeda, The innate immuneresponse to Trypanosoma cruzi infection, Microbes Infect. 12 (2010) 511–517.
[28] M. Ginger, Trypanosomatid biology and euglenozoan evolution: new insights and shifting paradigms revealed through genome sequencing, Protist 156 (2005) 377–392.
[29] J.J. Cazzulo, Aerobic fermentation of glucose by trypanosomatids, FASEB J. 6 (1992) 3153–3161.
[30] F. Bringaud, L. Riviere, V. Coustou, Energy metabolism of trypanosomatids: adaptation to available carbon sources, Mol. Biochem. Parasitol. 149 (2006) 1–9.
[31] I.G. Kirkinezos, C.T. Moraes, Reactive oxygen species and mitochondrial diseases, Cell Dev. Biol. 12 (2001) 449–457.